Annals of Biomedical Engineering

Development of an In Vitro 3D Brain Tissue Model Mimicking In Vivo-like Pro-inflammatory and Pro-oxidative Responses

--Manuscript Draft--

Manuscript Number:	ABME-D-17-00800R1
Full Title:	Development of an In Vitro 3D Brain Tissue Model Mimicking In Vivo-like Pro-inflammatory and Pro-oxidative Responses
Article Type:	Original Article
Keywords:	Collagen hydrogel; Microglia; Lipopolysaccharide; Reactive oxygen species; Cytokines.
Corresponding Author:	Yong Woo Lee, Ph.D. Virginia Tech Blacksburg, VA UNITED STATES
Corresponding Author Secondary Information:	
Corresponding Author's Institution:	Virginia Tech
Corresponding Author's Secondary Institution:	
First Author:	Hyung Joon Cho, Ph.D.
First Author Secondary Information:	
Order of Authors:	Hyung Joon Cho, Ph.D.
	Scott S. Verbridge, Ph.D.
	Rafael V. Davalos, Ph.D.
	Yong Woo Lee, Ph.D.
Order of Authors Secondary Information:	
Funding Information:	
Abstract:	To analyze complex inflammatory responses in an in vitro system, we constructed a new 3D in vitro brain tissue model that exhibits in vivo-like tissue responses (e.g. immune cell phenotypes, and molecular response) to inflammatory stimuli. Finite element modeling of oxygen diffusion and cellular oxygen consumption predicted the oxygen profile within 3D structures, consisting of Type I collagen hydrogel embedded with murine microglia. Viability and cytotoxicity analyses supported the mathematical analysis, determining optimal cell growth conditions for 3D construct development. Real-time RT-PCR and ELISA demonstrated significant up-regulation of pro-inflammatory mediators, such as TNF-α, MCP-1, IL-6 and IL-1β, in lipopolysaccharide (LPS)-stimulated in vitro cell culture (2D and 3D) and in vivo mouse model systems. Interestingly, levels of inflammatory responses from the in vitro 3D model system were more similar to in vivo than in vitro 2D. Additionally, in situ dihydroethidium (DHE) assay and immunofluorescence staining revealed that levels of LPS-stimulated reactive oxygen species (ROS) generation and microglial activation from in vitro 3D model system were closer to in vivo than in vitro 2D. These results demonstrated that an in vitro 3D model provides more physiologically relevant pro-oxidative and pro-inflammatory environments in brain than an in vitro 2D model.
Author Comments:	I am delighted to submit the manuscript, entitled "Development of an In Vitro 3D Brain Tissue Model Mimicking In Vivo-like Pro-inflammatory and Pro-oxidative Responses", to the Annals of Biomedical Engineering. In the present study, we have developed an in vitro 3D brain inflammation model system by encapsulating microglia within a collagen hydrogel matrix. Additionally, we have validated that an in vitro 3D model provides more physiologically relevant pro-oxidative and pro-inflammatory environments in brain than the traditional in vitro 2D model regarding oxygen profile of culture systems. To the best our knowledge, this is the first report comparing molecular

	and cellular responses among in vitro 2D, in vitro 3D and in vivo models in order to create a physiologically relevant in vitro 3D brain inflammation model. I declare that this manuscript, or part of it, neither has been published nor is currently under consideration for publication by any other journals. All animal protocols used have been approved by the authors' institutional animal experimentation committee. In addition, all authors listed have contributed to the work and have agreed to submit the manuscript. Should you have any questions or further assistance regarding this manuscript, please address them to me at (540) 231-8484 or at ywlee@vt.edu. Sincerely, Yong W. Lee, Ph.D. Associate Professor Department of Biomedical Engineering and Mechanics Virginia Tech, Blacksburg, VA 24061, USA
Additional Information:	
Question	**Response**
Please state the number of words in your manuscript including references.	5992

Development of an *In Vitro* 3D Brain Tissue Model Mimicking *In Vivo*-like Pro-inflammatory and Pro-oxidative Responses

HYUNG JOON CHO[1], SCOTT S. VERBRIDGE[2], RAFAEL V. DAVALOS[2], and YONG W. LEE[2]

[1]Department of Biochemistry and Molecular Biology, University of Miami Miller School of Medicine, Miami, FL 33136, USA; and [2]Department of Biomedical Engineering and Mechanics, Virginia Tech, Blacksburg, VA 24061, USA

An abbreviated title: *In vitro* 3D brain inflammation model

Corresponding author: Yong W. Lee, Ph.D., Department of Biomedical Engineering and Mechanics, 337 Kelly Hall (MC-0298), 325 Stanger Street, Virginia Tech, Blacksburg, VA 24061, USA. Tel: +1 (540) 231-8484. Fax: +1 (540) 231-9738. E-mail: ywlee@vt.edu

Abstract - To analyze complex inflammatory responses in an *in vitro* system, we constructed a new 3D *in vitro* brain tissue model that exhibits *in vivo*-like tissue responses (e.g. immune cell phenotypes, and molecular response) to inflammatory stimuli. Finite element modeling of oxygen diffusion and cellular oxygen consumption predicted the oxygen profile within 3D structures, consisting of Type I collagen hydrogel embedded with murine microglia. Viability and cytotoxicity analyses supported the mathematical analysis, determining optimal cell growth conditions for 3D construct development. Real-time RT-PCR and ELISA demonstrated significant up-regulation of pro-inflammatory mediators, such as TNF-α, MCP-1, IL-6 and IL-1β, in lipopolysaccharide (LPS)-stimulated *in vitro* cell culture (2D and 3D) and *in vivo* mouse model systems. Interestingly, levels of inflammatory responses from the *in vitro* 3D model system were more similar to *in vivo* than *in vitro* 2D. Additionally, *in situ* dihydroethidium (DHE) assay and immunofluorescence staining revealed that levels of LPS-stimulated reactive oxygen species (ROS) generation and microglial activation from *in vitro* 3D model system were closer to *in vivo* than *in vitro* 2D. These results demonstrated that an *in vitro* 3D model provides more physiologically relevant pro-oxidative and pro-inflammatory environments in brain than an *in vitro* 2D model.

Key Terms - Collagen hydrogel, Microglia, Lipopolysaccharide, Reactive oxygen species, Cytokines

INTRODUCTION

Three-dimensional (3D) cell culture methods provide researchers an opportunity to control temporal and spatial aspects of the tissue microenvironment, including cellular composition, concentrations and gradients of soluble factors as well as the extracellular matrix (ECM), enabling careful study of cellular behaviors under physiologically relevant and *in vivo*-like conditions.[6] Specifically, a 3D cell culture system has been shown to be a more accurate experimental model compared with the *in vivo* biology than a 2D cell culture due to various benefits. For example, *in vitro* 3D cell culture systems mimic *in vivo*-like cytostructures, delivering better knowledge of cell-cell and cell-matrix interactions.[7,11] In addition, *in vitro* 3D cell culture systems provide a higher surface area for cell growth and migration, which may promote cell survival and responses to extracellular cues.[11,20] Furthermore, *in vitro* 3D cell culture systems may provide protection from environmental disturbances by providing physiologically stable structures.[8] Moreover, cells encapsulated within *in vitro* 3D cell culture systems exhibit an amoeboid shape, which is the more physiologically relevant morphology, while cells growing in *in vitro* 2D cell culture systems yield only the less relevant flat and stretched shape.[11,22,28]

Hydrogels have been broadly explored for their ability to provide a distinctive and attractive matrix for ECM development, due to their excellent cellular capabilities of mimicking biochemical and mechanical properties of *in vivo* microenvironments.[24] Particularly, hydrogels formed from type I collagen have been a popular 3D scaffold with several excellent properties. Collagen is a cytocompatible, natural polymer in tissues and the most abundant protein in mammals. In addition, collagen plays a key role in cell

adhesion to ECM by presenting several integrin-binding sites, such as an arginine-glycine-aspartic acid sequence, and provides self-assembling capability to construct fibrillar structures in physiological environments.[10,16,20] Furthermore, collagen hydrogels are useful for investigating the effects of physical activation triggers.[13]

Despite considerable progress in the development of *in vitro* 3D tissue engineering with biomimetic hydrogels, there is still limited information linking nutrient transport to cellular distribution in the field of tissue-engineered 3D cell culture systems. The interaction between 3D scaffolds and metabolic demand (e.g. oxygen and glucose) is crucial in sustaining a functional cellular microenvironment in 3D cell culture systems. Given that oxygen is essential in maintaining the existence of all multicellular organisms through its role in cellular metabolism, proliferation, migration, differentiation, and cell-cell interactions,[26] failure to attain dynamic equilibrium of essential oxygen demand in time and space through tissue-engineered 3D constructs may result in non-functional tissues. Indeed, previous study emphasized that insufficient supply of nutrients including oxygen throughout the 3D system may lead to impairing engineered tissues.[12] Particularly, a few experimental trials of 3D culturing microglia, the primary immune cells in the central nervous system (CNS),[17] have been attempted to capture inflammatory responses in the brain[14,22,25]. While previous studies indicated that microglia play a critical role in pathological variations of the brain microenvironment and subsequent CNS injuries and neurodegenerative diseases,[15,19] limited information of oxygen profile is available in functional 3D microglial culture systems.

In this study, we developed an *in vitro* 3D model containing microglia, determined molecular and cellular responses after treatment with pro-oxidative and pro-inflammatory

Commented [CHJ1]: As the reviewer suggested, the part that may mislead readers about the role of oxygen profile in 3D culture system was removed.

stimulus, and compared them with conventional *in vitro* 2D and *in vivo* model systems. We combined this with careful control over the oxygen levels to ensure recapturing a physiologically relevant and *in vivo*-like brain inflammation model system.

MATERIALS AND METHODS

Cell Culture

The murine microglia, BV-2, was kindly provided from Dr. Michael E. Robbins (Wake Forest University Medical Center, Winston-Salem, NC) and cells were cultured in Dulbecco's modified eagle medium (DMEM; Hyclone Laboratories, Inc., Logan, UT) with 5% fetal bovine serum (FBS; Mediatech, Inc., Manassas, VA) containing 100 unit/ml of penicillin, and 100 µg/ml of streptomycin. Cells were cultured at 37°C with 5% CO_2 and 95% air under a humid atmosphere. To stimulate microglia into an inflammatory phenotype, cells were incubated with 100 ng/ml of lipopolysaccharide (LPS; Sigma-Aldrich, St. Louis, MO) for 4 and 24 h to investigate molecular and cellular changes, respectively.

Preparation of an In Vitro 3D Collagen Hydrogel and 3D Cell Culture

Type I collagen extracted from rat tails was used to construct an *in vitro* 3D structure. Briefly, 0.1 ml of type I collagen stock solution (1.5% w/v in 0.1% v/v acetic acid) was neutralized with 0.002 ml of NaOH (Sigma-Aldrich) and 0.025 ml of 10× DMEM (Sigma-Aldrich) on ice. The appropriate volume of concentrated cell suspension containing microglia in 0.123 ml of 1× DMEM was then mixed into the neutralized collagen solution. The collagen solution with cells was then placed into 24 well-plate by

polydimethylsiloxane (PDMS) wells, creating cylindrical collagen structures with 4-mm diameter and 2-mm thick, and allowed to polymerize at 37°C with 5% CO_2 for 30 min (Figure 1). After polymerization, collagen hydrogels including microglia were incubated with cell culture medium.

Animals and Tissue Collection/Preparation

Eight-week-old male C57BL/6 mice were purchased from The Jackson Laboratory (Bar Harbor, ME). Animals were maintained under environmentally controlled conditions and subject to a 12 h light/dark cycle with food and water *ad libitum*. All protocols in this study were approved by the Institutional Animal Care and Use Committee and were conducted in accordance with the National Institutes of Health Guide for the Care and Use of Laboratory Animals. To generate pro-oxidative and pro-inflammatory environments in the brain, mice were intraperitoneally injected with a single dose of LPS (0.5 mg/kg) in 0.2 ml of saline. Control groups only received 0.2 ml of saline.

Animals at 4 and 24 h following exposure to LPS or saline (n=5 per group) were briefly anesthetized with isoflurane (3%) and transcardially perfused with ice-cold phosphate-buffered saline (PBS) containing 6 unit/ml heparin. Two hemispheres of brains were then dissected following the rapid whole brain removal, immediately frozen in dry ice, and stored at −80°C until analysis; the hippocampus of left hemispheres was dissected for real-time RT-PCR analysis and ELISA. The right hemispheres were cryopreserved in 30% sucrose solution for 24 h and processed in Tissue-Tek® optimal cutting temperature (O.C.T.) embedding medium (Sakura Finetek USA, Inc., Torrance, CA). Serial 20 μm-

thick sagittal sections were prepared for *in situ* ROS detection and immunofluorescence staining.

Oxygen Consumption Rate and Finite Element Modeling

The basal cellular O_2 consumption was measured using an XF24 extracellular flux analyzer (Seahorse Bioscience, North Billerica, MA). Briefly, cells were seeded into 24-well plates (XF24 cell culture microplates) at 3 × 10^4 cells per well for 24 h in growth media. Prior to the assay, the culture medium was replaced with DMEM without sodium bicarbonate and phenol red, and placed in an incubator without CO_2 for 1 h. The dissolved oxygen in the medium surrounding the cells was then measured by solid-state fluorescence sensors, and oxygen consumption rate of microglia was calculated. The oxygen concentration levels within 3D hydrogels were initially estimated using a mathematical model with an assumption of consumption kinetics as zeroth order. Therefore, the oxygen consumption $\left[R\left(C_{O_2}\right);\ mol/m^3 \cdot s\right]$ of cells was treated depending on the spatial cell density $[\rho_{Cell};\ cells/ml]$ and oxygen consumption rate by cells $\left[R_{O_2,cell}\ ;\ mol/cell \cdot s\right]$ using the following simplified equation, $R\left(C_{O_2}\right) = \rho_{Cell} R_{O_2,cell}$. In addition, the population of cells over time was predicted by logistic cell growth.

$$N\ (t) = \rho_{Cell} \cdot V_{3D\ construct} = \frac{KN_0}{N_0 + (K - N_0)e^{-rt}}$$

where $N\ (t)$ is the cell number as a function of time (t), $V_{3D\ construct}\ [m^3]$ is the 3D hydrogel volume, K is the carrying capacity, $N_0\ [cells]$ is the initial cell seeding number, and $r\ [h^{-1}]$ is the cell growth rate. Estimated parameters of logistic cell growth, K and r, were experimentally predicted using MATLAB software (The MathWorks, Inc., Natick,

MA). Along with consumption kinetics and logistic cell growth, the final cross-sectional oxygen profile was computed by solving the following mass balance equation:

$$\frac{\partial C_{O_2}}{\partial t} = D\nabla^2 C_{O_2} - R\left(C_{O_2}\right)$$

where C_{O_2} $[mol/m^3]$ is the concentration of oxygen as a function of time (t) and position, and D $[m^2/s]$ is the oxygen diffusion constant for water. The partial pressure of oxygen (P_{O_2}) was calculated by using Henry's law and approximating the solubility of oxygen in water; $P_{O_2} = HC_{O_2}$ where H is the Henry's law constant for oxygen in water at 37°C: $H = 584.6$ $[m^3 \cdot mmHg/mol]$. The solution for oxygen profile within the 3D structure over time was calculated with the finite element modeling using commercial software package Comsol Multiphysics (Comsol Inc., Burlington, MA), assuming a fixed boundary concentration at 21% O_2 $\left[C_{O_2,0} = 273\ \mu M\right]$. The mesh was refined until error between successive refinements was smaller than 1% and the final mesh contained a total of 39,647 elements.

Live/Dead Viability/Cytotoxicity Assay

A LIVE/DEAD® Viability/Cytotoxicity kit (Molecular Probes, Eugene, OR) was used to determine viable/dead cell populations in 3D culture systems according to the protocol provided by the supplier. Briefly, after cell culture, 3D collagen hydrogels were rinsed with PBS twice and incubated in PBS containing calcein-AM (2 μM) and ethidium homodimer-1 (4 μM) at 37°C in 5% CO_2 for 45 min. After washing with PBS twice, live and dead cells were imaged by fluorescence microscopy.

Real-time Reverse Transcription-Polymerase Chain Reaction (RT-PCR)

Total RNA from *in vivo* and *in vitro* 3D model systems were isolated as described previously[29] while total RNA from *in vitro* 2D model system was isolated and purified using RNeasy Mini Kit (Qiagen, Valencia, CA) according to the protocol of the manufacturer. Quantitative real-time RT-PCR using TaqMan probes and primers were used for gene expression analyses. Amplification of individual genes was performed with Applied Biosystems 7300 real-time PCR system using TaqMan Universal PCR Master Mix and a standard thermal cycler protocol. TaqMan Gene Expression Assay Reagents for mouse pro-inflammatory genes, including tumor necrosis factor-α (TNF-α), monocyte chemoattractant protein-1 (MCP-1), interleukin-6 (IL-6), interleukin-1β (IL-1β), and glyceraldehyde 3-phosphate dehydrogenase (GAPDH, housekeeping gene) were used for specific probes and primers of PCR amplifications. The threshold cycle (C_T) was determined, and relative quantification was calculated by the comparative C_T method as described previously.[18]

Enzyme-linked Immunosorbent Assay (ELISA)

Cell culture supernatants from *in vitro* 2D model were collected after LPS stimulation while homogenates from mouse brains and *in vitro* 3D collagen hydrogels after LPS stimulation were prepared as described previously.[5] The protein expression levels of pro-inflammatory mediators in collected samples were determined by using Quantikine® Mouse Immunoassay Kits for TNF-α, MCP-1, IL-6, and IL-1β (R&D Systems, Minneapolis, MN) following the manufacturer's protocols. All targeted proteins were normalized by total protein amount (pg of target protein/mg of total protein) and LPS-treated group was compared by relative fold induction to untreated control group.

Commented [CHJ2]: As the reviewer suggested, the information related to protein normalization is added.

Immunofluorescence Staining

Frozen brain tissue sections (20 μm) were analyzed by immunofluorescence staining as described previously.[5] The primary antibody, rabbit anti-Iba1 (1:200), and its corresponding secondary antibody, goat anti-rabbit IgG conjugated with Alexa Fluor 555 (1:400), were utilized to detect Iba1 protein expression. Samples were mounted with a mounting medium with DAPI, imaged and quantified as described previously.[5] Integrated fluorescence intensity of samples was normalized by untreated control group (control=1) and relative changes of fluorescence intensity in LPS-treated groups were quantified.

Commented [CHJ3]: As the reviewer suggested, the information related to fluorescence intensity normalization is added.

In Situ Detection of Reactive Oxygen Species (ROS)

In situ levels of superoxide anion, the main species of ROS, were measured by *in situ* dihydroethidium (DHE) fluorescence staining. Briefly, brain sections were washed with PBS and incubated with 5 μM DHE solution in a light-protected humidified chamber at 37°C for 30 min. After incubation, the slides were rinsed with PBS and imaged with a Zeiss AXIO Imager A1m fluorescence microscope. Fluorescence intensity of acquired digital images was quantified by ImageJ software and relative changes of fluorescence intensity in LPS-treated groups compared to untreated control group were calculated.

Commented [CHJ4]: As the reviewer suggested, the information related to fluorescence intensity normalization is added.

Statistical Analysis

Statistical analysis of data was completed using SigmaPlot version 11 software (SPSS, Chicago, IL). A two-tailed student's t-test was applied to compare controls and experimental groups. A statistical probability (p) value of <0.05 was considered significant.

RESULTS

Design and Construction of an In Vitro 3D Collagen Hydrogel with Microglia

To explore the contribution of spatial dimension on cellular and molecular responses, an *in vitro* 3D model comprised of microglia-seeded 2 mm-thick type I collagen hydrogel was engineered. The basal oxygen consumption of microglia was measured by the XF24 analyzer; $R_{O_2,cell} = 6.78 \times 10^{-17} mol/cell \cdot s$. Assuming cell clusters were uniformly distributed within the engineered 3D hydrogel, finite element modeling of the steady-state oxygen distribution within the 3D structure was performed with the values of initial cell seeding density, measured oxygen consumption $(R_{O_2,cell})$, and oxygen diffusion coefficient (D) in water (Figure 2A). As shown in Figure 2B, three different oxygen concentration distributions at the point probe $(z = 0, r = 0)$ were uniformly maintained after 30 min depending on initial cell seeding densities; 20.2% at $5 \times 10^5\ cells/ml$, 19.4% at $1 \times 10^6\ cells/ml$, and 17.8% at $2 \times 10^6\ cells/ml$, respectively. In addition, cross-sectional oxygen concentration distributions after 1 h were predicted according to the initial cell seeding densities (Figure 2D). Oxygen concentration distribution with logistic cell growth over time was also computed. As depicted in Figure 2C, three different profiles of partial pressure of O_2 (%) were predicted during 72 h depending on initial cell seeding densities and correspondingly estimated values of carrying capacity (K) and cell growth rate (r). After 72 h, partial pressure of O_2 (%) dramatically dropped down below 1% (0.9%) in the 3D hydrogel of the initial cell seeding density with $2 \times 10^6\ cells/ml$ while remaining above 5% with the initial cell seeding density of $5 \times 10^5\ cells/ml$ and $1 \times 10^6\ cells/ml$. Furthermore, cross-sectional oxygen concentration distributions of different cell seeding

Commented [CHJ5]: As the reviewer's suggestion, the sentence is revised using the word 'cell clusters'.

densities demonstrated that higher cell density yielded a greater range of oxygen gradient within the 3D hydrogel matrix (Figure 2E).

In addition to mathematical modeling analyses, fluorescence microscopy with live/dead viability/cytotoxicity assay was employed to visualize the distribution of viable and dead cells within 3D constructs after incubation of 48, 72, and 96 h (Figure 3A). Quantitative analysis of live and dead cells in fluorescence intensity demonstrated that the 3D construct with the initial cell seeding density of $1 \times 10^6\ cells/ml$ and 72 h of cell growth showed the highest viability and lowest cytotoxicity (Figure 3B). Therefore, based on mathematical modeling analyses and live/dead viability/cytotoxicity assay, the optimal culture conditions, such as the initial cell seeding density of $1 \times 10^6\ cells/ml$ and 72 h of cell growth, were selected to study physiologically relevant microglial responses within 2 mm-thick engineered 3D structures.

Pro-inflammatory Responses of an In Vitro 3D System after LPS Stimulation

To compare the pro-inflammatory responses among *in vitro* 2D, *in vitro* 3D and *in vivo* model systems, mRNA expression levels of pro-inflammatory mediators, such as TNF-α, MCP-1, IL-6 and IL-1β, were determined by quantitative real-time RT-PCR after 4 h of LPS stimulation. As shown in Figure 4, a significant up-regulation of TNF-α, MCP-1, IL-6 and IL-1β expressions was observed in LPS-treated groups. Expression of GAPDH (a housekeeping gene), however, was not affected by LPS stimulation (data not shown). In particular, cells grown on *in vitro* 2D system exhibited much higher inflammatory responses to LPS treatment (41.02-fold induction of TNF-α, 50-fold induction of MCP-1, 43,158-fold induction of IL-6, and 2,198-fold induction of IL-1β; $p<0.05$) than those in cells

grown on *in vitro* 3D system (24-fold induction of TNF-α, 35-fold induction of MCP-1, 721-fold induction of IL-6, and 237-fold induction of IL-1β; $p<0.05$) and *in vivo* system (9-fold induction of TNF-α, 12-fold induction of MCP-1, 3.92-fold induction of IL-6, and 17-fold induction of IL-1β; $p<0.05$). In addition, protein expression levels of TNF-α, MCP-1, IL-6 and IL-1β after LPS stimulation were quantified by ELISA (Figure 5). A markedly higher up-regulation of protein expressions of pro-inflammatory mediators after LPS stimulation was detected in cells grown on *in vitro* 2D system (64-fold induction of TNF-α, 22-fold induction of MCP-1, 99-fold induction of IL-6, and 8.4-fold induction of IL-1β; $p<0.05$) compared with cells grown on *in vitro* 3D system (7.1-fold induction of TNF-α, 10-fold induction of MCP-1, 46-fold induction of IL-6, and 7.8-fold induction of IL-1β; $p<0.05$) and *in vivo* system (4.7-fold induction of TNF-α, 3.9-fold induction of MCP-1, 11-fold induction of IL-6, and 5.5-fold induction of IL-1β; $p<0.05$). These results demonstrated that the pro-inflammatory responses in cells grown on *in vitro* 3D system are lower than those in cells grown on *in vitro* 2D system and are closer to *in vivo* system, indicating that the *in vitro* 3D model system, newly developed in the present study, produces more physiologically relevant pro-inflammatory environments in brain than the traditional *in vitro* 2D model system.

Pro-oxidative Responses of an In Vitro 3D System after LPS Stimulation

To compare the pro-oxidative responses among *in vitro* 2D, *in vitro* 3D and *in vivo* model systems, *in situ* DHE fluorescence staining was performed to detect ROS generation after 4 h of LPS stimulation. A significant increase of superoxide anion in LPS-treated groups was measured and compared to each control group (Figure 6A-6F).

Quantitative analysis of fluorescence intensity exhibited that LPS treatment significantly enhanced ROS generation by 24-fold (*in vitro* 2D), 7.8-fold (*in vitro* 3D), and 14-fold (*in vivo*), respectively (Figure 6G). These results demonstrated that the pro-oxidative responses in cells grown on the *in vitro* 3D system are lower than those in cells grown on the *in vitro* 2D system and are closer to the *in vivo* system, indicating that the *in vitro* 3D model system, newly developed in the present study, produces more physiologically relevant pro-oxidative environments in the brain than traditional *in vitro* 2D model systems.

Microglial Activation of an In Vitro 3D System after LPS Stimulation

To compare microglial activation among *in vitro* 2D, *in vitro* 3D and *in vivo* models after 24 h of LPS treatment, the protein expression levels of Iba1, a microglial activation marker, were visualized by immunofluorescence staining. A significantly increased number of Iba1-immunopositive cells was detected in LPS-treated groups compared to each control group (Figure 7A-7F). Quantitative analysis of fluorescence intensity demonstrated that LPS treatment significantly increased the number of activated microglia by 9.1-fold (*in vitro* 2D), 1.7-fold (*in vitro* 3D), and 2.4-fold (*in vivo*), respectively (Figure 7G). These results demonstrated that the *in vitro* 3D model, produces more physiologically relevant levels of microglial activation in brain than traditional *in vitro* 2D model.

DISCUSSION

The rapid progress in tissue engineering and biotechnology has provided new strategies for investigating complex physiological and pathophysiological processes in

the body. A variety of tools for growing cells in 3D architectures have been expanded over the past decade to create functional *in vitro* 3D experimental models. Indeed, a number of previous studies have demonstrated that *in vitro* 3D models have the potential to improve understanding of more relevant cellular physiology and pathology than traditional 2D models.[12,28] For example, 3D cell culture systems mimic physiologically relevant microenvironments by providing mechanical properties, such as stiffness, molecular composition of the ECM, and information delivery of cell-to-cell and cell-to-matrix interactions and regulations of cellular behaviors and responses.[7,11,22]

One main challenge to designing 3D cell culture systems is the limited information regarding nutrient delivery and cellular distribution for maintaining function and viability. Particularly, oxygen is normally considered to be a limiting factor due to its low solubility in culture medium while gradients in glucose and amino acids are almost negligible. Compared with conventional 2D cell culture systems, *in vitro* 3D systems may result in differentially proliferating regions of cells due to different oxygen gradients (diffusion) within the 3D constructs. In addition, cell density linked to temporal oxygen gradients may determine cells' fate in the 3D structures according to metabolic oxygen consumption of cells. Previous studies have emphasized that understanding of the spatial oxygen gradient established in 3D constructs depending on cell density is crucial to balancing oxygen diffusion and cellular metabolism (oxygen consumption).[2,27,30] The present study investigated the magnitude of oxygen concentration distribution throughout the 3D construct using a mathematical analysis in terms of diffusion (oxygen diffusion) and reaction (oxygen consumption). Computational simulations predicted the oxygen diffusion through a 3D cylindrical collagen structure and oxygen consumption by seeded microglia.

In addition, experimentally obtained logistic microglial growth was integrated into the mathematical model to further estimate oxygen distribution profile within the construct depending on cellular growth over time, adding the part of oxygen consumption according to cellular proliferation. Our results showed that, according to initial cell seeding densities, oxygen concentration within the construct fell towards each approximate equilibrium and remained with relatively high partial pressure of O_2 (%) ranging from 17 to 20 after the first 30-min simulation. However, oxygen distribution dramatically dropped as the cells proliferated afterwards within the 3D constructs with the highest cell density, which may result in oxygen depletion.

The oxygen concentrations in tissues are much lower than the atmospheric oxygen concentrations (about 21% partial pressure of O_2); a range of 2 to 10% is frequently observed in mammalian tissues. In particular, previous *in vivo* and clinical studies measuring oxygen concentration indicated that the partial pressure of oxygen in brain tissue above 5% is a normoxic condition in the brain.[1,4] In contrast, pathological hypoxia with values below 1% resulted in compromised cellular metabolism *in vivo*.[21] In the present study, the initial cell seeding density of 5×10^5 cells/ml and 1×10^6 cells/ml remained above 5% partial pressure of O_2 throughout the 3D constructs after 72-h growth (namely, ~15% with the initial cell seeding density of 5×10^5 cells/ml and ~9% with 1×10^6 cells/ml) while the construct with the initial cell seeding density of 2×10^6 cells/ml underwent pathological hypoxia condition. To further optimize the culturing conditions of *in vitro* 3D system and support the mathematical analyses, live/dead viability/cytotoxicity assays were conducted. These results demonstrated that the 3D construct with initial cell seeding density of 1×10^6 cells/ml and 72-h growth period exhibited the highest viability

and lowest cytotoxicity within the system (by the maximum slope line in mean green fluorescence intensity over mean red fluorescence intensity). Therefore, these experimental parameters were selected to develop a model of "normal" (e.g. normoxic) immune-responsive brain tissue for this study. Although these selected conditions meet normoxic tissue levels in the current study, cell density should be explored for different oxygen profiles depending on cell types.

To investigate molecular and cellular responses of the *in vitro* 3D model system, LPS stimulation was employed to create pro-oxidative and pro-inflammatory environments in microglia. LPS has been widely used to trigger pro-oxidative and pro-inflammatory pathways and microglial responses to LPS have been well characterized.[3] The present study demonstrated that molecular and cellular responses of *in vitro* 3D and *in vivo* model systems after LPS stimulation were much lower than those observed in *in vitro* 2D system. Previous studies also showed differential (or diminished) molecular and cellular responses of 3D cell cultures, including gene expression,[9] cell cycle progression and its regulating signaling pathway,[23] and inflammation,[14,25] upon various stimulus in comparison to the cells cultured in 2D systems. These results imply that oxygen diffusion may be limited in *in vitro* 3D and *in vivo* systems compared with *in vitro* 2D system due to the presence of oxygen diffusion barrier, such as hydrogels and tissues. However, more detailed analyses regarding attachment substrates (e.g. uncoated *vs.* collagen-coated monolayer cell culture) are required to observe whether cell attachment can cause different responses to LPS in three different culture systems.

Interestingly, pro-oxidative responses and microglial activation of *in vivo* system after LPS stimulation were higher than those of *in vitro* 3D system. This result may be due to

Commented [CHJ6]: Additional information was added to better understand the Figure 3B.

Commented [CHJ7]: According to the reviewer's suggestion, this sentence is added as our limitation in the current study.

the presence of vasculature *in vivo* to continuously provide oxygen into tissues. To our knowledge, similar studies have not been conducted with models based on tissue-resident immune cell types regarding oxygen profile of 3D cell culture, and furthermore there has been a dearth of comparison of inflammatory profiles with *in vivo* models.

Collagen and hyaluronic acid (HA) are two widely used natural hydrogel materials in the recent development of 3D culture systems. Particularly, HA have been drawn recent attention, given its principal role in the formation of brain ECM by interacting with cell surface receptors, activating various signaling pathways, and regulating cell behaviors, such as growth, migration of certain types of cells (e.g. neurons and astrocytes) and differentiation. However, HA requires further modifications (with its broad spectrum of molecular weights and variation in modifications) to support specific crosslinking mechanisms between cells and ECM while collagen provides cell adhesion without modification plus tunable viscoelastic environment to resident cells; therefore, collagen was selected as our hydrogel material for the 3D cultures. However, the current study requires further expansion on designing hydrogel materials (e.g. HA-based scaffolds) to more accurately recreate the intricate structural and mechanical milieus of the brain ECM and address the potential role of cell-ECM interactions (e.g. regulation of inflammatory signaling).

In summary, we have developed an *in vitro* 3D brain inflammation model system by encapsulating microglia within a collagen hydrogel matrix. Although an *in vitro* 3D model system in the current study is a simplified structure with the single cell type (microglia) compared to intricate brain possessing other important cell types, such as neurons and astrocytes, we have validated that an *in vitro* 3D model provides more physiologically

Commented [CHJ8]: As the reviewer commented, the limitation of the current in vitro 3D model with single cell type (microglia) was addressed compared to other important brain cell types, such as neurons and astrocytes.

relevant pro-oxidative and pro-inflammatory environments in brain than the traditional *in vitro* 2D model regarding oxygen profile of culture systems. To the best our knowledge, this is the first report comparing molecular and cellular responses among *in vitro* 2D, *in vitro* 3D and *in vivo* models in order to create a physiologically relevant *in vitro* 3D brain inflammation model.

ACKNOWLEDGMENTS

The authors are thankful to Nabil Boutagy, Ph.D., Department of Medicine, Yale University School of Medicine, for his vital assistance with the Seahorse XF24 analyzer.

REFERENCES

[1]Almendros, I., J. M. Montserrat, M. Torres, C. González, D. Navajas, and R. Farré. Changes in oxygen partial pressure of brain tissue in an animal model of obstructive apnea. Respir. Res. 11:3, 2010.

[2]Ardakani, A. G., U. Cheema, R. A. Brown, and R. J. Shipley. Quantifying the correlation between spatially defined oxygen gradients and cell fate in an engineered three-dimensional culture model. J. R. Soc. Interface 11:20140501, 2014.

[3]Block, M. L., L. Zecca, and J. S. Hong. Microglia-mediated neurotoxicity: uncovering the molecular mechanisms. Nat. Rev. Neurosci. 8:57-69, 2007.

[4]Carreau, A., B. El Hafny-Rahbi, A. Matejuk, C. Grillon, and C. Kieda. Why is the partial oxygen pressure of human tissues a crucial parameter? Small molecules and hypoxia. J. Cell. Mol. Med. 15:1239-1253, 2011.

[5]Cho, H. J., V. S. Sajja, P. J. Vandevord, and Y. W. Lee. Blast induces oxidative stress, inflammation, neuronal loss and subsequent short-term memory impairment in rats. Neuroscience 253:9-20, 2013.

[6]Cox, M. C., L. M. Reese, L. R. Bickford, and S. S. Verbridge. Toward the broad adoption of 3D tumor models in the cnacer drug pipeline. ACS Biomater. Sci. Eng. 1:877-894, 2015.

[7]Cukierman, E., R. Pankov, D. R. Stevens, and K. M. Yamada. Taking cell-matrix adhesions to the third dimension. Science 294:1708-1712, 2001.

[8]Cullen, D. K., J. A. Wolf, V. N. Vernekar, J. Vukasinovic, and M. C. LaPlaca. Neural tissue engineering and biohybridized microsystems for neurobiological investigation in vitro (Part 1). Crit. Rev. Biomed. Eng. 39:201-240, 2011.

[9]DelNero, P., M. Lane, S. S. Verbridge, B. Kwee, P. Kermani, B. Hempstead, A. Stroock, and C. Fischbach. 3D culture broadly regulates tumor cell hypoxia response and angiogenesis via pro-inflammatory pathways. Biomaterials 55:110-118, 2015.

[10]Fang, M., E. L. Goldstein, E. K. Matich, B. G. Orr, and M. M. Holl. Type I collagen self-assembly: the roles of substrate and concentration. Langmuir 29:2330-2338, 2013.

[11]Geckil, H., F. Xu, X. Zhang, S. Moon, and U. Demirci. Engineering hydrogels as extracellular matrix mimics. Nanomedicine (Lond) 5:469-484, 2010.

[12]Griffith, L. G., and M. A. Swartz. Capturing complex 3D tissue physiology *in vitro*. Nat. Rev. Mol. Cell. Biol. 7:211-224, 2006.

[13]Grinnell, F. Fibroblast biology in three-dimensional collagen matrices. Trends Cell. Biol. 13:264-269, 2003.

[14]Haw, R. T., C. K. Tong, A. Yew, H. C. Lee, J. B. Phillips, and S. Vidyadaran. A three-dimensional collagen construct to model lipopolysaccharide-induced activation of BV2 microglia. J. Neuroinflammation 11:134, 2014.

[15]Hu, X., A. K. Liou, R. K. Leak, M. Xu, C. An, J. Suenaga, Y. Shi, Y. Gao, P. Zheng, and J. Chen. Neurobiology of microglial action in CNS injuries: receptor-mediated signaling mechanisms and functional roles. Prog. Neurobiol. 119-120:60-84, 2014.

[16]Jokinen, J., E. Dadu, P. Nykvist, J. Käpylä, D. J. White, J. Ivaska, P. Vehviläinen, H. Reunanen, H. Larjava, L. Häkkinen, and J. Heino. Integrin-mediated cell adhesion to type I collagen fibrils. J. Biol. Chem. 279:31956-31963, 2004.

[17]Kettenmann, H., U. K. Hanisch, M. Noda, and A. Verkhratsky. Physiology of microglia. Physiol. Rev. 91:461-553, 2011.

[18]Lee, W. H., W. E. Sonntag, M. Mitschelen, H. Yan, and Y. W. Lee. Irradiation induces regionally specific alterations in pro-inflammatory environments in rat brain. Int. J. Radiat. Biol. 86:132-144, 2010.

[19]Luo, X. G., J. Q. Ding, and S. D. Chen. Microglia in the aging brain: relevance to neurodegeneration. Mol. Neurodegener. 5:12, 2010.

[20]O'Connor, S. M., D. A. Stenger, K. M. Shaffer, D. Maric, J. L. Barker, and W. Ma. Primary neural precursor cell expansion, differentiation and cytosolic Ca^{2+} response in three-dimensional collagen gel. J. Neurosci. Methods 102:187-195, 2000.

[21]Okazaki, K., and E. Maltepe. Oxygen, epigenetics and stem cell fate. Regen. Med. 1:71-83, 2006.

[22]Pöttler, M., S. Zierler, and H. H. Kerschbaum. An artificial three-dimensional matrix promotes ramification in the microglial cell-line, BV-2. Neurosci. Lett. 410:137-140, 2006.

[23]Riedl, A., M. Schlederer, K. Pudelko, M. Stadler, S. Walter, D. Unterleuthner, C. Unger, N. Kramer, M. Hengstschlager, L. Kenner, D. Pfeiffer, G. Krupitza, and H. Dolznig. Comparison of cancer cells in 2D vs 3D culture reveals differences in AKT-mTOR-S6K signaling and drug responses. J. Cell Sci. 130:203-218, 2017.

[24]Skardal, A., M. Devarasetty, H. W. Kang, I. Mead, C. Bishop, T. Shupe, S. J. Lee, J. Jackson, J. Yoo, S. Soker, and A. Atala. A hydrogel bioink toolkit for mimicking native tissue biochemical and mechanical properties in bioprinted tissue constructs. Acta Biomater. 25:24-34, 2015.

[25]Song, Q., Z. Jiang, N. Li, P. Liu, L. Liu, M. Tang, and G. Cheng. Anti-inflammatory effects of three-dimensional graphene foams cultured with microglial cells. Biomaterials 35:6930-6940, 2014.

[26]Stamati, K., V. Mudera, and U. Cheema. Evolution of oxygen utilization in multicellular organisms and implications for cell signalling in tissue engineering. J. Tissue Eng. 2:2041731411432365, 2011.

[27]Streeter, I., and U. Cheema. Oxygen consumption rate of cells in 3D culture: the use of experiment and simulation to measure kinetic parameters and optimise culture conditions. Analyst 136:4013-4019, 2011.

[28]Tibbitt, M. W., and K. S. Anseth. Hydrogels as extracellular matrix mimics for 3D cell culture. Biotechnol. Bioeng. 103:655-663, 2009.

[29]Toborek, M., Y. W. Lee, S. Kaiser, and B. Hennig. Measurement of inflammatory properties of fatty acids in human endothelial cells. Methods Enzymol. 352:198-219, 2002.

[30]Verbridge, S. S., N. W. Choi, Y. Zheng, D. J. Brooks, A. D. Stroock, and C. Fischbach. Oxygen-controlled three-dimensional cultures to analyze tumor angiogenesis. Tissue Eng. Part A 16:2133-2141, 2010.

FIGURE LEGENDS

FIGURE 1. Preparation of an *in vitro* 3D brain inflammation model system using type I collagen hydrogel with microglia.

FIGURE 2. Mathematical modeling of oxygen concentration distribution within 3D hydrogel. Finite element model of oxygen consumption within 3D model was computationally calculated, assuming the zeroth-order consumption kinetics: $D = 2.76 \times 10^{-9} m^2/s$, $C_{O_2,0} = 273\ \mu M$, $R_{O_2,cell} = 6.78 \times 10^{-17} mol/cell \cdot s$. In these computations, boundary conditions of oxygen concentration were maintained at the surface of 3D structure $\left(C_{O_2\ @z=2\ or\ r=2} = C_{O_2,0}\right)$ and no-flux conditions were maintained at the bottom of surface $(z = 0)$. Three different cell seeding densities were applied for the calculation; $5 \times 10^5 cells/ml$, $1 \times 10^6 cells/ml$, and $2 \times 10^6 cells/ml$. (A) Schematic of *in vitro* 3D hydrogel; (B) Prediction of O_2 partial pressure (%) at the point probe during the first 60 min; (C) Prediction of O_2 partial pressure (%) at the point probe during 72 h with logistic cell growth; (D) Prediction of cross-sectional O_2 levels after 60 min; (E) Prediction of cross-sectional O_2 levels after 72 h.

FIGURE 3. Live/dead cell viability/cytotoxicity assay by fluorescence microscopy. The fluorescence intensity of live and dead cells within the 3D hydrogel was visualized by

LIVE/DEAD® viability/cytotoxicity assay kit. (A) Representative images of live and dead cells within 3D hydrogels at 1 mm-depth varying cell densities and culture periods. (B) Quantitative analysis of fluorescence intensity of live and dead cells within 3D hydrogels. Data represent mean ± SEM for each group (n=3). Scale bar: 1,000 μm.

FIGURE 4. Comparison of the mRNA expression levels of pro-inflammatory mediators among *in vitro* 2D, *in vitro* 3D and *in vivo* model systems after LPS stimulation. The mRNA expression levels of TNF-α (A), MCP-1 (B), IL-6 (C), and IL-1β (D) were measured by quantitative real-time RT-PCR. Data represent mean ± SEM for each group (n=4). *p<0.05 vs. each control group.

FIGURE 5. Comparison of the protein expression levels of pro-inflammatory mediators among *in vitro* 2D, *in vitro* 3D and *in vivo* model systems after LPS stimulation. The protein expression levels of TNF-α (A), MCP-1 (B), IL-6 (C), and IL-1β (D) were determined by ELISA. Data represent mean ± SEM for each group (*in vitro* 2D and *in vitro* 3D: n=6; *in vivo*: n=5). *p<0.05 vs. each control group.

FIGURE 6. Comparison of the levels of ROS generation among *in vitro* 2D, *in vitro* 3D and *in vivo* model systems after LPS stimulation. The fluorescence intensity of superoxide anion was visualized by *in situ* DHE staining. (A) Control (*in vitro* 2D); (B) LPS stimulation (*in vitro* 2D); (C) Control (*in vitro* 3D); (D) LPS stimulation (*in vitro* 3D); (E) Control (*in vivo*); (F) LPS stimulation (*in vivo*); (G) Quantitative analysis of fluorescence intensity. Data represent mean ± SEM for each group (*in vitro* 2D and *in vitro* 3D: n=6; *in vivo*: n=5).

*p<0.05 vs. each control group. Scale bar: (A) and (B), 200 μm; (C) and (D), 1,000 μm; (E) and (F), 100 μm.

FIGURE 7. Comparison of the levels of microglial activation among *in vitro* 2D, *in vitro* 3D and *in vivo* model systems after LPS stimulation. The levels of microglial activation were visualized by Iba1-positive immunofluorescence staining. (A) Control (*in vitro* 2D); (B) LPS stimulation (*in vitro* 2D); (C) Control (*in vitro* 3D); (D) LPS stimulation (*in vitro* 3D); (E) Control (*in vivo*); (F) LPS stimulation (*in vivo*); (G) Quantitative analysis of fluorescence intensity. Data represent mean ± SEM for each group (*in vitro* 2D: n=4; *in vitro* 3D and *in vivo*: n=5). *p<0.05 vs. each control group. Scale bar: (A) and (B), 100 μm; (C) and (D), 1,000 μm; (E) and (F), 50 μm.

Figure 1

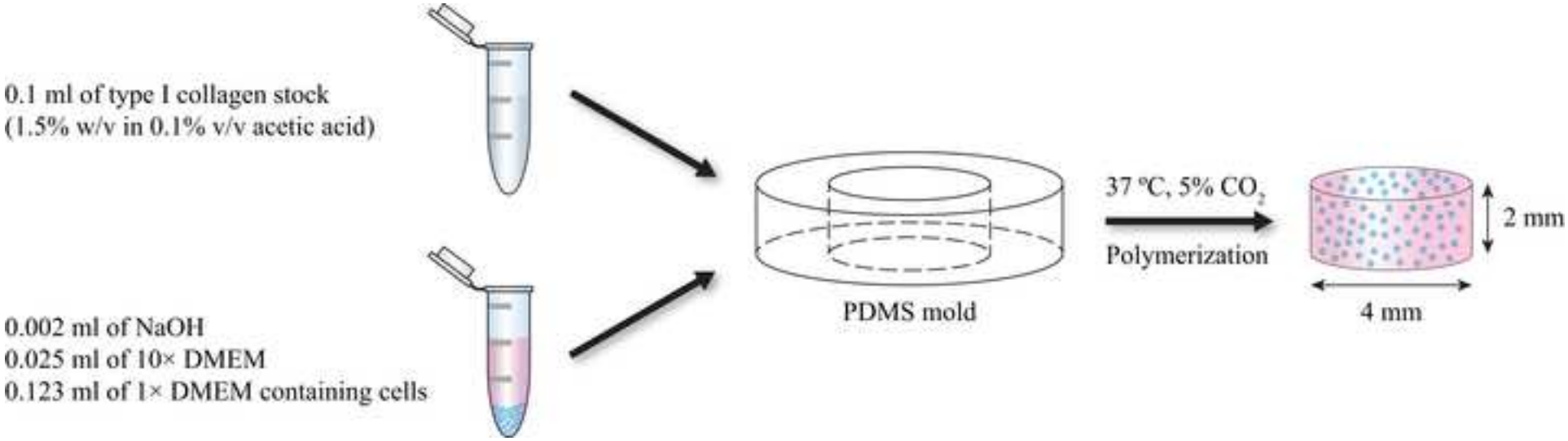

Figure 2

Click here to download Figure Fig2.tif

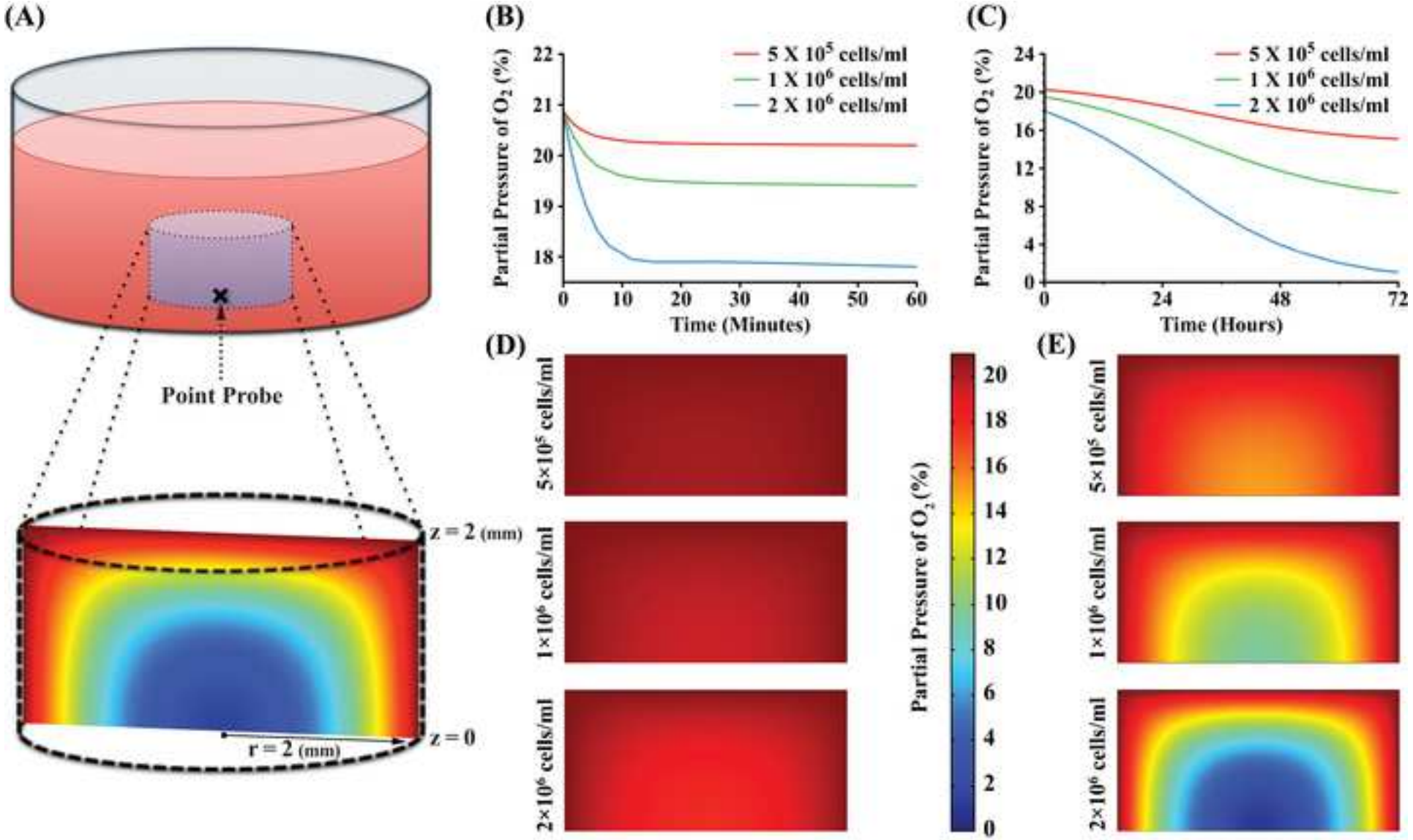

Figure 3

Click here to download Figure Fig3-New.tif

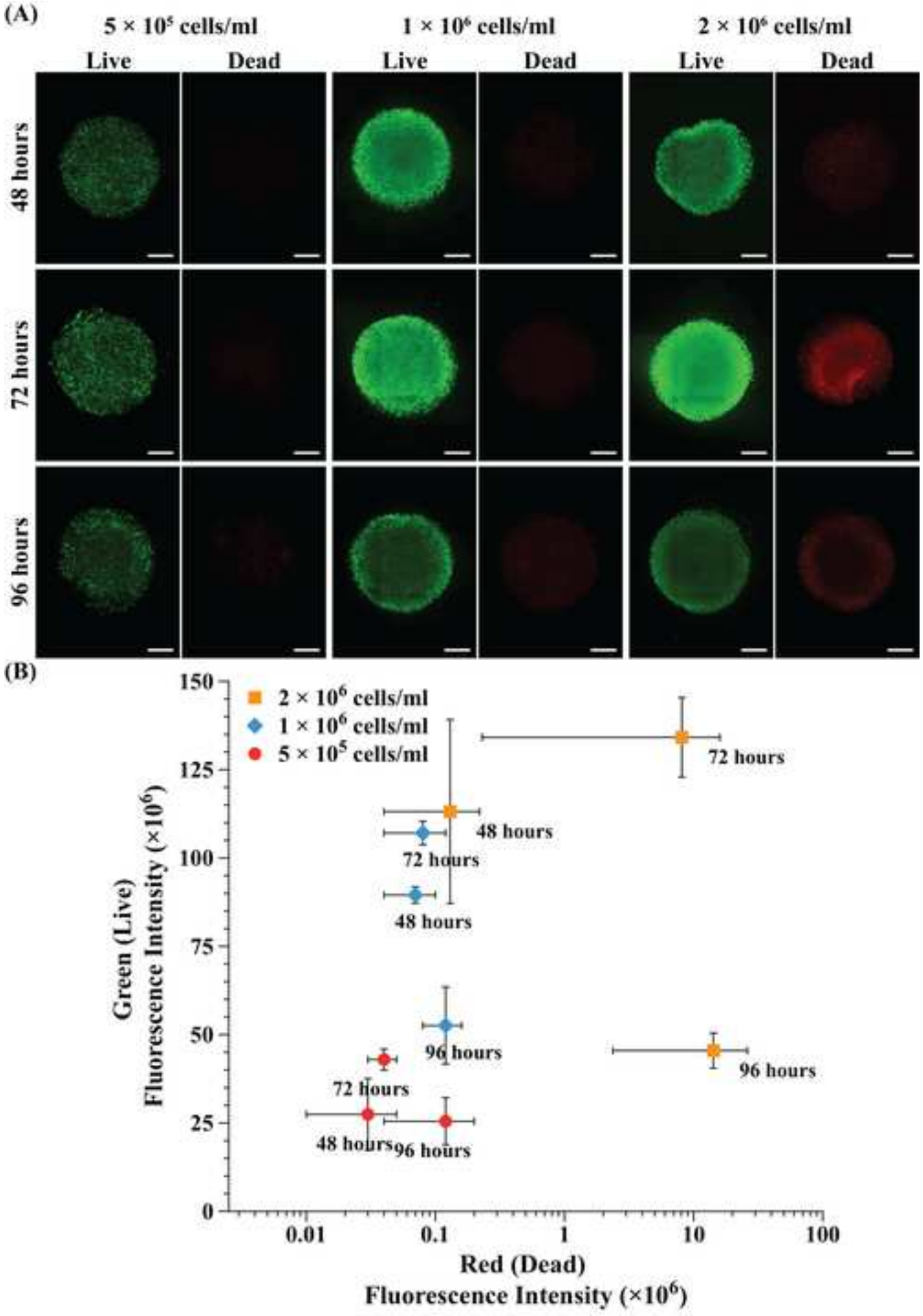

Figure 4

Click here to download Figure Fig4.tif

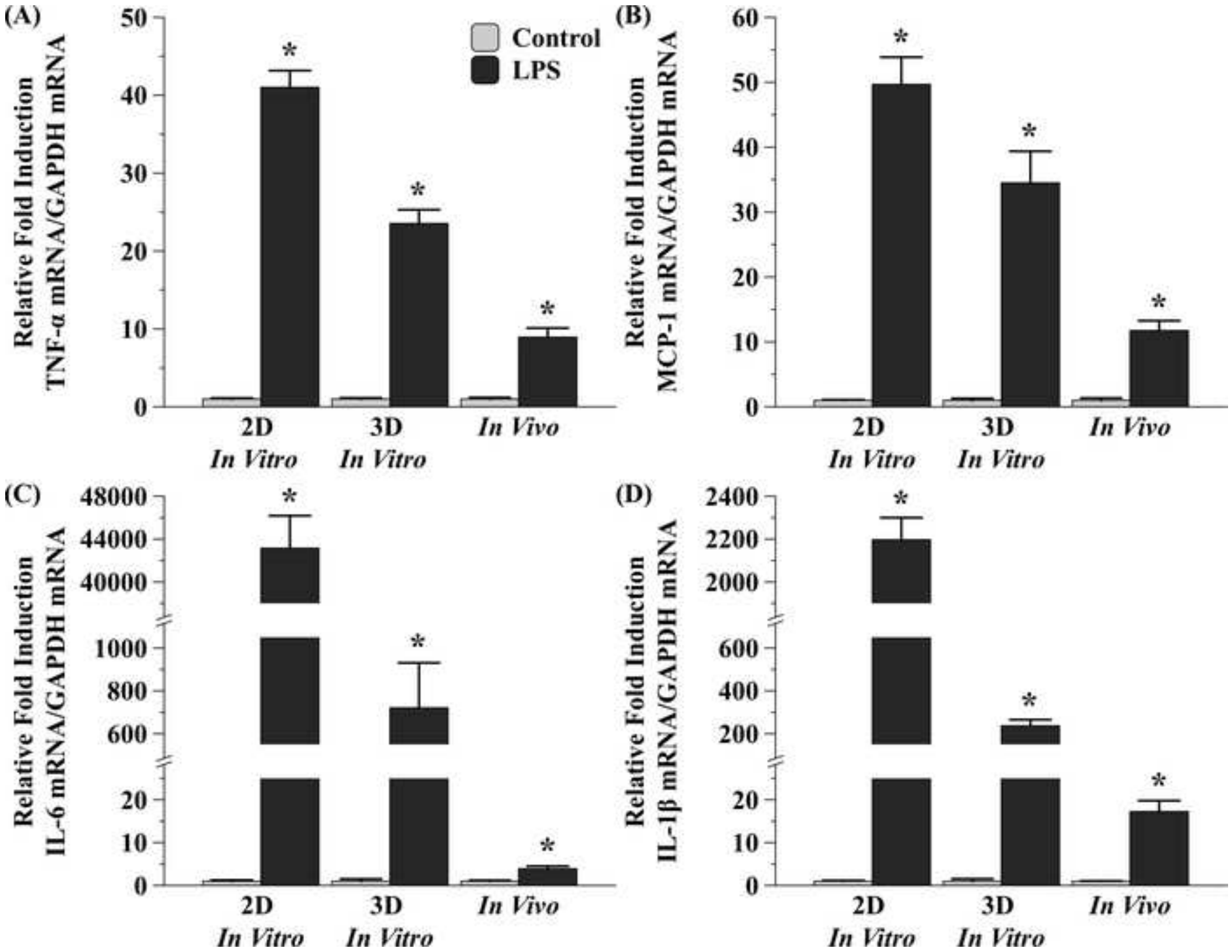

Figure 5

Click here to download Figure Fig5.tif

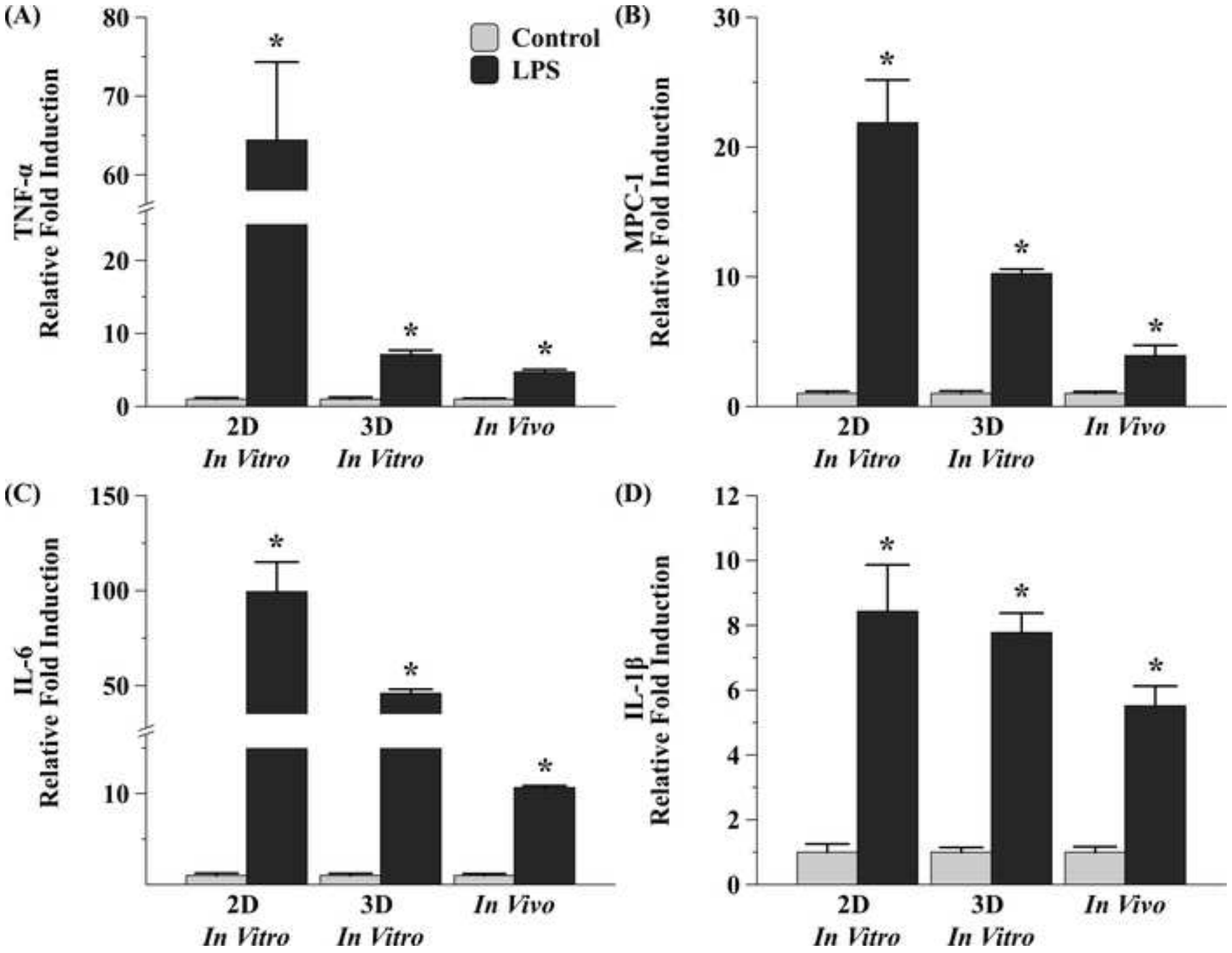

Figure 6

Click here to download Figure Fig6.tif

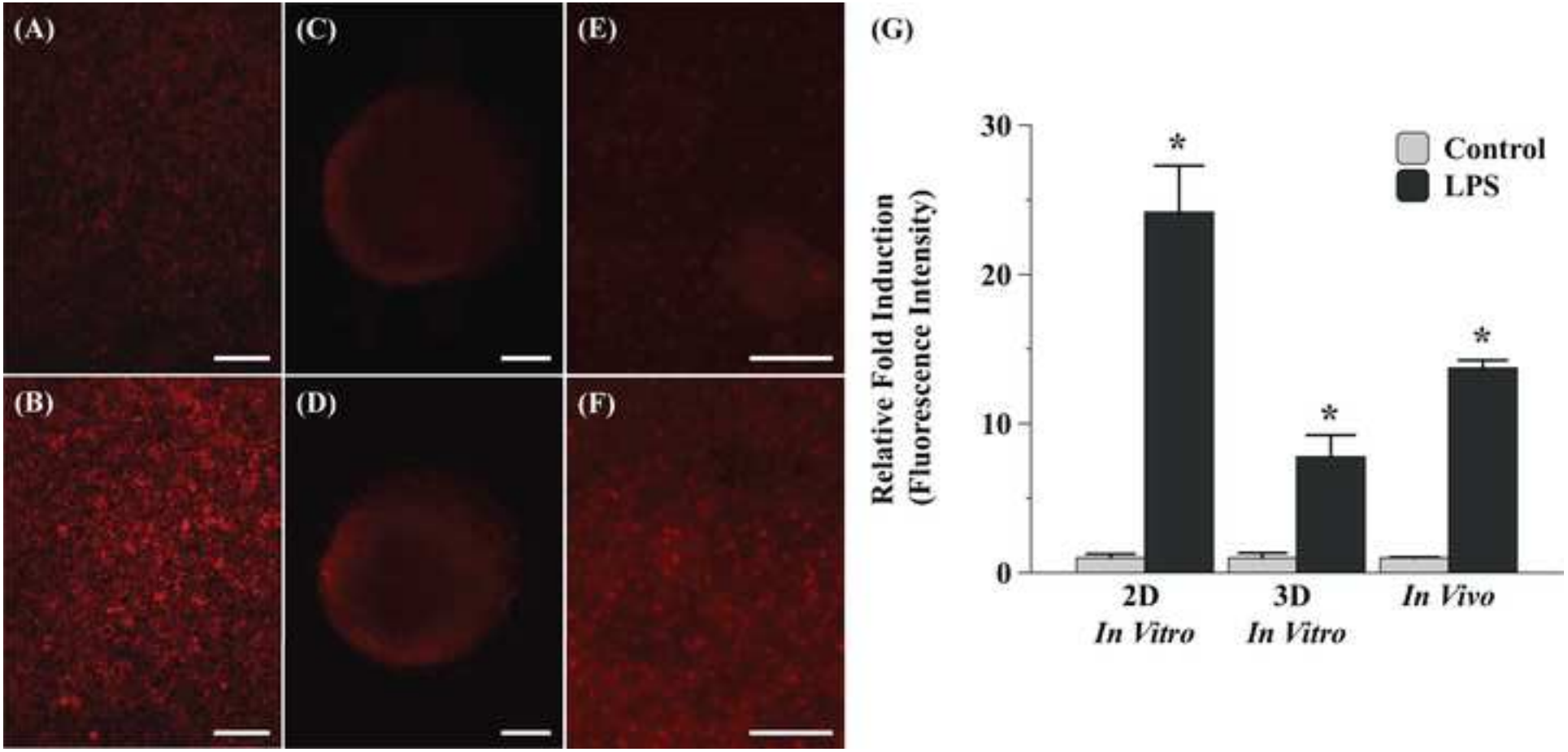

Figure 7

Click here to download Figure Fig7.tif